Int Urol Nephrol (2017) 49:215–224
DOI 10.1007/s11255-016-1460-3

UROLOGY - ORIGINAL PAPER

Renal cell carcinoma: applicability of the apparent coefficient of the diffusion-weighted estimated by MRI for improving their differential diagnosis, histologic subtyping, and differentiation grade

Yulian Mytsyk[1] · Ihor Dutka[2] · Yuriy Borys[1] · Iryna Komnatska[2] · Iryna Shatynska-Mytsyk[3] · Ammad Ahmad Farooqi[4] · Katarina Gazdikova[5,6] · Martin Caprnda[7] · Luis Rodrigo[7] · Peter Kruzliak[8,9]

Received: 25 August 2016 / Accepted: 10 November 2016 / Published online: 16 November 2016

Abstract
Background Renal cell carcinoma (RCC) represents the most common malignant epithelial neoplasm of the kidney. Accurate assessment of the renal masses, defining the histologic subtype and the grade of differentiation of the tumor, is vital to ensure an adequate case management as well as for staging and prognosis. Recently, diffusion-weighted imaging (DWI) magnetic resonance imaging (MRI) tends to be increasingly appealing for the clinicians as an imaging procedure of choice for the diagnosis and staging of the RCC, which is predetermined by several advantages over CT. The goal of the survey was to assess the applicability of the apparent diffusion coefficient (ADC) of the DWI MRI for the differential diagnostics, histologic subtyping, and defining the grade of differentiation of the RCC.
Methods The study enrolled 288 adult patients with renal lesions: 188 patients with solid RCC—126 patients with clear cell subtype (ccRCC), 32 patients with papillary RCC (pRCC), 30 patients with chromophobe RCC (chRCC); 27 patient with cystic form or RCC (Bosniak cyst, category IV); 32 patients with renal angiomyolipoma (AML); 25 patients with renal oncocytoma (OC); and 16 patients with the renal abscess (AB). In total, 245 lesions were pathologically verified. As a reference, 19 healthy volunteers were included into the study. All patients underwent MRI of the kidneys, involving DWI with subsequent evaluation of the ADC.
Results There was a reliable difference ($p < 0.05$) in mean ADC values between the normal renal parenchyma (NRP), solid RCC of different histologic subtypes and grades, cystic RCC, and benign renal lesions. The mean ADC values obtained in the result of the study were ($\times 10^{-3}$ mm^2/s): 2.47 ± 0.12 in NRP, 1.63 ± 0.29 in all solid RCCs, 1.82 ± 0.22 in solid ccRCC (1.92 ± 0.11—Fuhrman grade I, 1.84 ± 0.14—Fuhrman grade II, 1.79 ± 0.10—Fuhrman grade III, 1.72 ± 0.06—Fuhrman grade IV), 1.61 ± 0.07 in pRCC, 1.46 ± 0.09 in chRCC, 2.68 ± 0.11 in cystic RCC, 2.13 ± 0.08 in AML, 2.26 ± 0.06 in OC, and 3.30 ± 0.07 in AB.

✉ Yulian Mytsyk
mytsyk.yulian@i.ua

✉ Katarina Gazdikova
katarina.gazdikova@szu.sk

✉ Peter Kruzliak
kruzliakpeter@gmail.com

[1] Department of Urology, Lviv National Medical University, Pekarska str. 69, Lviv, Ukraine

[2] Euroclinic Medical Center, Lviv, Ukraine

[3] Department of Radiology, Lviv National Medical University, Lviv, Ukraine

[4] Laboratory of Translational Oncology and Personalized Medicine, Rashid Latif Medical College, Lahore, Pakistan

[5] Department of Nutrition, Faculty of Nursing and Professional Health Studies, Slovak Medical University, Limbova 12, 833 03 Bratislava, Slovak Republic

[6] Department of General Medicine, Faculty of Medicine, Slovak Medical University, Bratislava, Slovak Republic

[7] University of Oviedo, Central University Hospital of Asturias (HUCA), Oviedo, Spain

[8] Department of Chemical Drugs, Faculty of Pharmacy, University of Veterinary and Pharmaceutical Sciences, Palackeho tr 1946/1, 612 42 Brno, Czech Republic

[9] 2nd Department of Surgery, Faculty of Medicine, Masaryk University, Brno, Czech Republic

Conclusion The data received in our study demonstrate a substantial restriction of diffusion of hydrogen molecules in tissues of ccRCC in comparison with the healthy renal parenchyma preconditioned by the greater density of tumor. A statistically significant difference in mean ADC values of ccRCC with different grades of nuclear pleomorphism by Fuhrman was observed: Low-grade tumors showed higher mean ADC values compared to high-grade tumors. The modality of the MRI DWI along with ADC measurement allows to reliably differentiate between the solid RCC of main histologic subtypes and grades, cystic RCC, and the benign renal lesions.

Keywords Renal cell carcinoma · Magnetic resonance imaging · Diffusion-weighted imaging · Apparent diffusion coefficient

Abbreviations

AB	Renal abscess
ADC	Apparent diffusion coefficient
AML	Angiomyolipoma
ccRCC	Clear cell renal cell carcinoma
chRCC	Chromophobe renal cell carcinoma
CT	Computed tomography
DWI	Diffusion-weighted images
FIESTA FAT SAT	Fast imaging employing steady-state acquisition with fat saturation
FRFSE	Fast-recovery fast spin-echo
FSPGR-DE	Fast spoiled gradient-recalled echo dual-echo
LAVA	Liver acquisition with volume acquisition
MRI	Magnetic resonance imaging
NRP	Normal renal parenchyma
OC	Oncocytoma
pRCC	Papillary renal cell carcinoma
RCC	Renal cell carcinoma
RCC	Renal cell carcinoma
ROI	Region of interest
SNR	Signal-to-noise ratio
SSFSE	Single-shot fast spin-echo
TE	Echo time
TR	Repetition time

Introduction

Renal cell carcinoma (RCC) is responsible for about 3% of all cancers in adults and 90% of all renal tumors. Over the last 10 years, a substantial increase in the incidence of the latter tumor is observed as supported by statistical data. Large-scale study, SEER (Surveillance, Epidemiology and End Results), had revealed that approximately 1 in 69 males and 1 in 116 females during their lifetime would be diagnosed with RCC [1].

Accurate assessment of the renal masses, defining the RCC histologic subtype and the grade of differentiation of the tumor, is vital to ensure an adequate case management as well as for staging and prognosis [2]. Recently, computed tomography (CT) and magnetic imaging resonance (MRI) are the primary imaging tools for diagnosing, evaluating, and staging of the renal masses. The density or intensity on unenhanced imaging and the enhancement characteristics have been employed for the elucidation of the renal mass nature [3]. Lately, the differences in enhancement characteristics of clear cell RCC (ccRCC) and papillary RCC (pRCC) have been described [4, 5]. With the implementing of multichannel coils and parallel imaging, functional analysis has become available, providing superior temporal and spatial resolution. Despite these advances, there are many cases, for which imaging modalities cannot readily provide an easy differentiation of the benign and malignant lesions. Recent studies have demonstrated that 16–33% of nephrectomies are performed on benign lesions [6]. Diffusion-weighted imaging (DWI) represents an MRI modality employing strong bipolar gradients in order to create a sensitivity of the signal to the thermally induced Brownian motion (or random walk) of water molecules and enabling in vivo measurement of molecular diffusion [7]. The apparent diffusion coefficient (ADC) is a quantitative parameter calculated from DWI images, which is applied as a measure of diffusion. Recent studies evaluated the significance of DWI in renal masses evaluation and obtained comprehensive data on morphologic and functional state of the kidney [8–10]. With regard to recently reported concerns about nephrogenic systemic fibrosis occurrence in patients with renal insufficiency which previously had contrast-enhanced MRI and given the risk of contrast material-induced nephropathy with contrast-enhanced CT, there is an emerging attention toward non-enhancing imaging modalities which might be valuable for characterizing renal lesions [11, 12]. The purpose of our study was to assess the significance of DWI in differentiating benign and malignant solid kidney tumors.

The goal of the survey was to assess the applicability of the apparent diffusion coefficient (ADC) of the diffusion-weighted imaging (DWI) MRI for the differential diagnostics, histologic subtyping, and defining the grade of differentiation of the RCC.

Materials and methods

The imaging results were obtained from the database of the Urology Department of Lviv National Medical University and from the database of the Euroclinic Medical Center,

Lviv, Ukraine, during the period of 2013–2016 and were endorsed by local Ethics Committee.

Retrospective study was conducted involving 288 adult patients with renal lesions (111 males and 177 females, aged 40–75 years, mean age 56.1 ± 2.9 years): 188 patients with solid RCC—126 patients with clear cell histologic subtype of RCC (ccRCC, Fuhrman grade I—27 patients, Fuhrman grade II—43 patients, Fuhrman grade III—35 patients, Fuhrman grade IV—21 patient), 32 patients with papillary RCC (pRCC), 30 patients with chromophobe RCC (chRCC); 27 patient with cystic form or RCC (Bosniak cyst, category IV, all patients with clear cell subtype, Fuhrman grade I—5 patients, Fuhrman grade II—14 patients, Fuhrman grade III—6 patients, Fuhrman grade IV—2 patients); 32 patients with renal angiomyolipoma (AML, lipid poor $n = 7$, lipid rich $n = 25$); 25 patients with renal oncocytoma (OC); and 16 patients with the renal abscess (AB). All patients with solid and cystic RCCs and OC had undergone partial ($n = 38$) or radical ($n = 202$) nephrectomy with subsequent pathological verification of diagnosis. According to clinical indications in 3 patients with AML (constant gross hematuria) and in 2 patients with AB (insufficient medicament therapy), surgical treatment—partial nephrectomy—was performed. In total, 245 lesions were pathologically verified.

Prospective data analysis was performed in control group that consisted of 19 healthy volunteers without known renal disease according to clinical examinations (anamnesis, physical examination, complete blood count, urinalysis, biochemistry of blood) and ultrasonography data (9 men and 10 women) aged 22–48 years (mean age 45.6 ± 3.9 years). The study included the results of examinations of all participants who met the inclusion and exclusion criteria from the above medical facilities. Exclusion criteria were as follows: patients with renal insufficiency or metal parts in the body; no DWI series; poor quality of DW image with apparent artifacts. Anticancer treatment in patients prior to the MRI and surgery was not performed. MR imaging was performed with a 1.5 T body scanner (Signa HDxt, General Electric, USA) using an 8-channel phased-array body coil. MR Imaging Protocol for renal masses included standard GE series and additionally axial DWI with the following parameters: TR = 12,000 ms, TE = 90 ms, field of view = 40 cm × 40 cm; matrix = 200 × 192; NEX = 3; bandwidth = 250 kHz, diffusion direction = slice, slice thickness = 6.0 mm, interscan gap = 1.0 mm with b values = 0 and 800 mm^2/s), acquisition time = 17 s. DWI was performed prior to contrast media administration (gadopentetate dimeglumine, in a dose of 0.1 mmol/kg of body weight as a bolus injection), using single-shot echo-planar imaging sequence with parallel imaging technique and fat saturation during one breath-hold.

Image analysis

Image interpretation was done qualitatively by visual evaluation of the DWI images and the corresponding ADC map, and quantitatively by measuring the ADC value of the lesion. The signal intensity of the tumors on DWI was categorized as high-, iso-, and low-signal intensity when compared with contralateral parenchyma. Color ADC map was generated automatically at the workstation (Advantage Windows, GE Healthcare). The ADC was calculated with linear regression analysis of the function:

$$S = S0 * \exp(-b * ADC),$$

Table 1 Lesion characteristics

Pathologic type/grade	Cases	Mean size (cm, mean ± SD)	M	F	Median age (years, mean ± SD)
Normal renal parenchyma	19	–	9	10	45.6 ± 3.9
All solid RCCs	188	6.0 ± 2.0	67	121	60.6 ± 3.3
Clear cell RCC	126	6.3 ± 1.9	41	85	57.1 ± 2.7
Fuhrman grade I	27	4.2 ± 1.8	10	17	54.5 ± 3.7
Fuhrman grade II	43	4.5 ± 1.6	15	28	59.2 ± 1.5
Fuhrman grade III	35	5.1 ± 1.9	16	19	58.6 ± 3.1
Fuhrman grade IV	21	6.3 ± 2.1	9	12	56.1 ± 2.3
Papillary RCC	32	5.1 ± 1.7	13	19	61.4 ± 3.2
Chromophobe RCC	30	6.5 ± 2.4	13	17	63.2 ± 3.9
Cystic RCC	27	7.1 ± 2.2	12	15	58.3 ± 2.7
Angiomyolipoma	32	5.9 ± 2.1	14	18	52.5 ± 2.4
Oncocytoma	25	4.4 ± 1.3	11	14	59.8 ± 3.6
Renal abscess	16	3.4 ± 1.4	7	9	49.1 ± 2.3
Total renal lesions	288	5.4 ± 1.8	111	177	56.1 ± 2.9

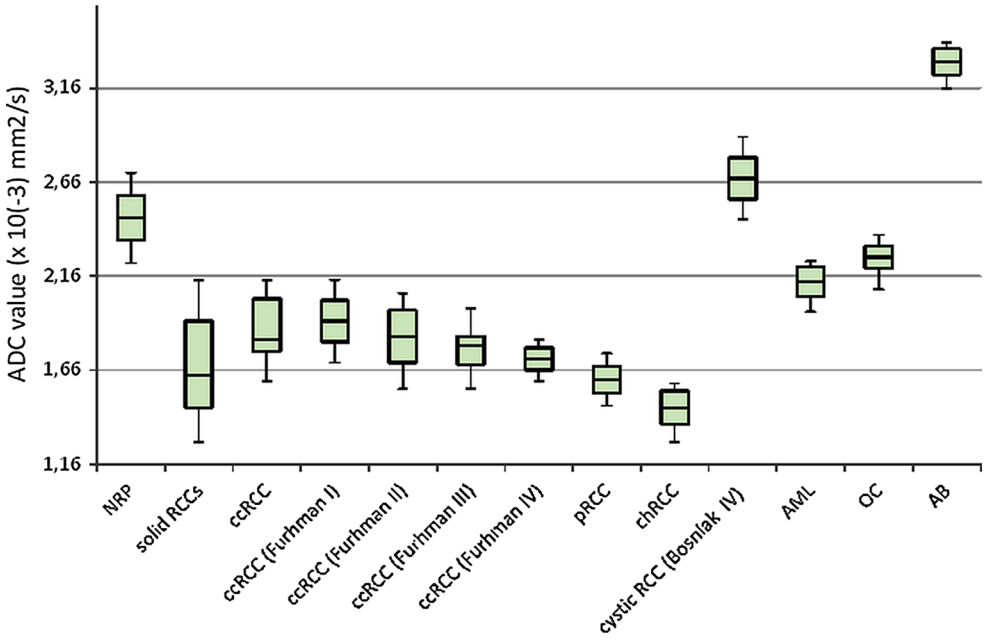

Fig. 1 Box-and-whisker plot of ADC values of the normal renal parenchyma, RCCs of different histologic subtypes and grades and of benign renal lesions. *Boxes* interquartile range, *whiskers* range of all values, *horizontal line within box* median ADC; *NRP* normal renal parenchyma, *ccRCC* clear RCC, *chRCC* chromophobe RCC, *pRCC* papillary RCC, *AML* angiomyolipoma, *OC* oncocytoma, *AB* renal abscess. Confidence interval (CI)—95%

where *S* is the signal intensity following the application of the diffusion gradient and *S*0 is the signal intensity on the DW image acquired at $b = 0$ s/mm^2.

The region of interest (ROI) was placed within a portion of the solid area where the minimum ADC value on the ADC map was registered consistent with the color by visual assessment. An average of two to three measurements was made per lesion, in accordance with the lesion volume. The mean ADC value was recorded within ROI. Necrotic regions were identified with conventional MRI sequences as regions of decreased contrast enhancement and avoided for ROI placement.

Statistical analysis

Functool software was applied for ADC map generation and measurements, and SPSS 22.0 software was used for data processing. The ADC value was expressed as mean + standard deviation. Results were considered statistically significant when p value was <0.05.

Results

All renal lesions had a diameter, which exceeded 2 cm, with an average size of 4.9 ± 2.4 cm ranging from 2.6 to 14.7 cm (Table 1). Malignant tumors had demonstrated mainly irregular shape on MRI images with irregular and indistinct outlines. All patients had monofocal tumors. Patients with solid RCC in 135 (71.81%) cases showed homogeneous signal; 53 patients (28.19%) had pronounced heterogeneous signal predetermined by the presence of necrotic component within the tumor.

Fig. 2 MRI of the patient, 65 years old, ccRCC of the left kidney, grade II of differentiation by Fuhrman (*arrows*). **a** Coronal T2-weighted single-shot fast spin-echo (SSFSE), repetition time (TR) = 2625 ms, echo time (TE) = 90 ms, flip angle (FA) = 90°, field of view (FOV) = 40 × 40 cm, matrix = 200 × 192; inhomogeneous hyperintensive tumor 45 × 36 × 33 mm of lower segment of the left kidney with hypointense pseudocapsule with ill-defined margins, **b** sagittal T2-weighted fast-recovery fast spin-echo (FRFSE), TR = 8750 ms, TE = 78 and 132 ms, FA = 90°, FOV = 44 × 44 cm, matrix = 384 × 192; hyperintensive tumor compresses calyces of lower segment of the left kidney, **c** axial T2-weighted SSFSE, hyperintensive tumor compresses and invades the calyces of lower segment of the left kidney, **d** axial T1-weighted fast spoiled gradient-recalled echo dual-echo (FSPGR-DE), TR = 130 ms, TE = 4.4 ms, FA = 70°, FOV = 43 × 43 cm, matrix = 320 × 192, breath-hold; tumor is represented as the hypointense region, **e** on axial DWI with b values = 0 and 800 mm^2/s tumor is represented as hyperintense region or the restricted diffusion, **f** ADC map, ROI over the tumor region showed the higher ADC value (1.82×10^{-3} mm^2/s)

The analysis of the yielded data had revealed that the average ADC value of solid malignant tumors was significantly lower compared to unaffected renal parenchyma and was $1.63 \pm 0.29 \times 10^{-3}$ versus $2.47 \pm 0.12 \times 10^{-3}$ mm^2/s, respectively ($p < 0.01$), due to significantly higher density of the RCC tissue and, consequently, due to the restriction of the hydrogen molecules diffusion within the tumor. Evaluation of the mean ADC value in patients with solid ccRCC of different degrees of malignancy consistent with classification by Fuhrman had demonstrated a decrease in the mean ADC value along with the increase in the nuclear polymorphism (Fig. 1). Therefore, in patients with grade I, the mean

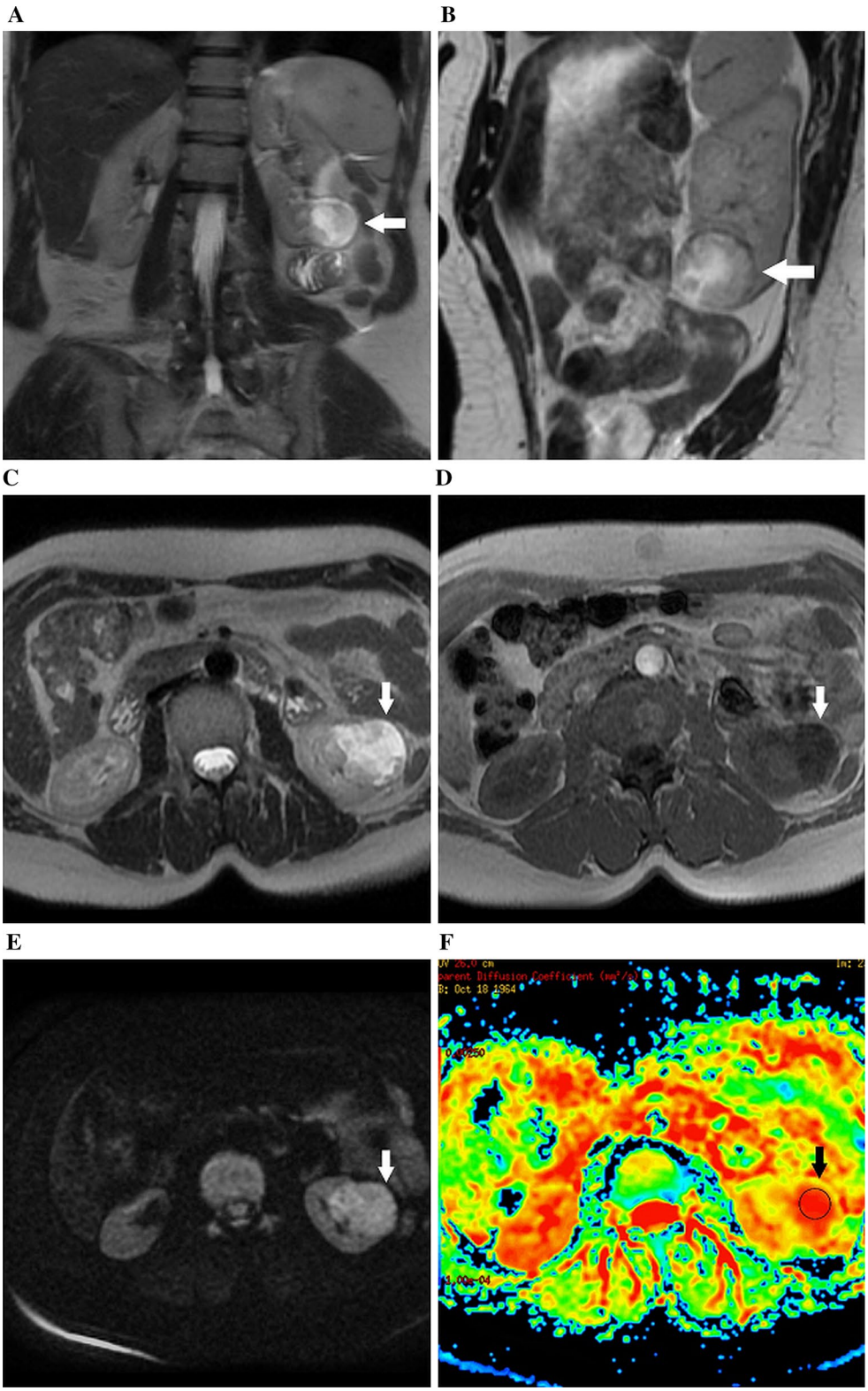

ADC value was 1.92 ± 0.11 × 10^{-3} mm^2/s, in patients with grade II, this value was 1.84 ± 0.14 × 10^{-3} mm^2/s (Fig. 2), in patients with grade III, the mean ADC value was 1.79 ± 0.10 × 10^{-3} mm^2/s, and in patients with grade IV of nuclear polymorphism, the mean ADC value was 1.72 ± 0.06 × 10^{-3} mm^2/s. Statistical comparison of the data received from patients with different degrees of ccRCC differentiation had revealed a significant difference

between groups ($p < 0.05$). These data indicate that malignant tumors are characterized by a severe restriction in the diffusion of hydrogen molecules within the tumor on DWI. We observed statistically reliable difference in mean ADC values of the benign and malignant renal tumors: In AML, mean ADC was $2.13 \pm 0.08 \times 10^{-3}$ mm^2/s (Fig. 3), in renal OC—$2.26 \pm 0.06 \times 10^{-3}$ versus $1.63 \pm 0.29 \times 10^{-3}$ mm^2/s in all solid RCCs ($p < 0.05$). The mean ADC values of normal renal parenchyma, RCCs of different histologic subtypes and grades and of benign renal lesions are shown in Table 2, and comparison between the groups of the patients is presented in Table 3.

Discussion

Recent studies have demonstrated the significance of the DWI MR with subsequent ADC measurement in the diagnosis of the RCC [10, 13, 14, 17–20].

In the result of our study, a statistically significant difference was observed between the mean ADC values of the normal renal parenchyma and solid ccRCC tumors: $2.47 \pm 0.12 \times 10^{-3}$ versus $1.63 \pm 0.29 \times 10^{-3}$ mm^2/s, respectively. The above data correlate with results obtained by other scientists: Wang et al. [13] used 3T MR imaging system and *b* values 0 and 800, the mean ADC values of the normal renal parenchyma and ccRCC were $2.30 \pm 0.17 \times 10^{-3}$ and $1.69 \pm 0.32 \times 10^{-3}$ mm^2/s, respectively. In our study, we used 1.5T imaging system, which may explain some differences in the obtained results between the studies. In another study, Razek et al. analyzed the ADC levels of the ccRCCs scanned on 1.5T MR system with *b* values of 0 and 800 and obtained the results that are comparable with these demonstrated in our study: The mean ADC value of the malignant tumors was $1.72 \pm 0.12 \times 10^{-3}$ mm^2/s. Additionally, authors had compared ADC levels of other histologic subtypes of the RCC and received significant difference. Unfortunately, this study lacks the data on the mean ADC levels of the unaffected renal parenchyma [14].

Precise characterization of the grades of differentiation of the ccRCC is vital for prognosis and management. The degree of malignancy of ccRCC is determined based on various histologic classifications. Recently, four-tiered Fuhrman grading system is the most commonly used for the determination of the degree of differentiation of ccRCC. In some recent works, the attempts to simplify this classification into three-tiered or even two-tiered system were made [15, 16]. Sandrasegaran et al. used two-tiered gradation system for the ccRCC in their study. In the result of the ADC data analysis of the patients with ccRCC (1.5T MR system and DWI with *b* values of 0 and 800 were used), authors received the difference in the ADCs of the low-grade and high-grade tumors. The mean ADC value of the low-grade tumors was higher than in high-grade lesions: $1.95 \pm 0.25 \times 10^{-3}$ versus $1.77 \pm 0.20 \times 10^{-3}$ mm^2/s, respectively. However, the results were statistically unreliable [10]. In our study, we used traditional four-tier Fuhrman grading system and achieved results had the same trend as in above study. Low differentiated ccRCCs (grades I and II) had highest ADC values compared to low differentiated (grades III and IV) lesions: For the grade I tumors, the mean ADC value was $.92 \pm 0.11 \times 10^{-3}$ mm^2/s, for the grade II tumors, this value was $1.84 \pm 0.14 \times 10^{-3}$ mm^2/s, the grade III lesions had the mean ADC value of $1.79 \pm 0.10 \times 10^{-3}$ mm^2/s, and in patients with grade IV of ccRCCs, the mean ADC value was $1.72 \pm 0.06 \times 10^{-3}$ mm^2/s. The obtained data were statistically significant ($p < 0.05$). The divergence in the mean ADC values in both studies can be explained by the different methodology of the ROI placement. In our study, we placed ROI exclusively within a portion of the solid area where the minimum ADC value on the ADC

Fig. 3 MRI of the patient, 52 years old, cystic RCC (Boslnak ▶ cyst class IV, Fuhrman grade II) of the left kidney (*arrows*). **a** Coronal T2-weighted SSFSE, repetition time (TR) = 2625 ms, echo time (TE) = 90 ms, flip angle (FA) = 90°, field of view (FOV) = 40 × 40 cm, matrix = 200 × 192; inhomogeneous hyperintense tumor 22 × 24 × 23 mm of the left kidney with irregularly thickened walls, pseudocapsule with no indices of infiltration into surrounding tissues, **b** axial T2-weighted SSFSE, TR = 2625 ms, TE = 94.1 ms, flip angle = 90°, field of view = 40 × 40 cm, matrix = 384 × 256; inhomogeneous hyperintense tumor of the left kidney with irregularly thickened walls, **c** on sagittal T2-weighted liver acquisition with volume acquisition (LAVA) with gadopentetate dimeglumine, TR = 3.5 ms, TE = 1.7 ms, flip angle = 90°, field of view = 40 × 40 cm, matrix = 256 × 192, inhomogeneous contrast enhancement of the peripheral region of the lesion, containing enhancing soft-tissue components, **d** axial T2-weighted LAVA with gadopentetate dimeglumine, TR = 3.5 ms, TE = 1.7 ms, flip angle = 90°, field of view = 40 × 40 cm, matrix = 256 × 192, inhomogeneous contrast enhancement of lesion, **e** on axial DWI with *b* values = 0 and 800 mm^2/s tumor is represented by inhomogeneous hyperintense region of restricted diffusion, **f** ADC map, ROI over the tumor region showed restricted diffusion—2.67×10^{-3} mm^2/s)

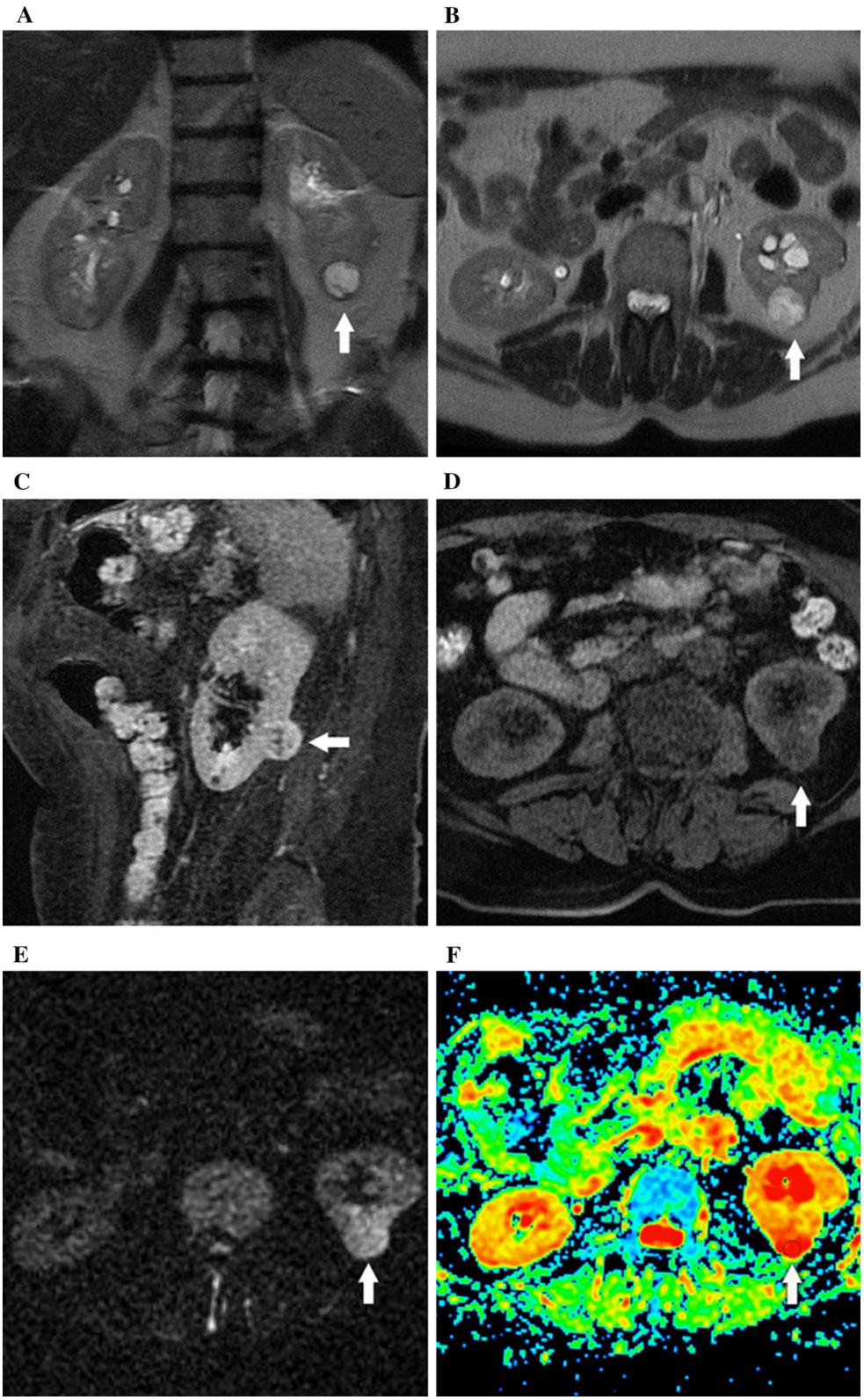
A
B
C
D
E
F

Table 2 Mean ADC values of normal renal parenchyma and RCC of different histologic subtypes and grades

Pathologic type/grade (cases)	Mean ADC value ($\times 10^{-3}$ mm^2/s)
Normal renal parenchyma (19)	2.47 ± 0.12
All solid RCCs (188)	1.63 ± 0.29
Clear cell RCC (126)	1.82 ± 0.22
Fuhrman grade I (27)	1.92 ± 0.11
Fuhrman grade II (43)	1.84 ± 0.14
Fuhrman grade III (35)	1.79 ± 0.10
Fuhrman grade IV (21)	1.72 ± 0.06
Papillary RCC (32)	1.61 ± 0.07
Chromophobe RCC (30)	1.46 ± 0.09
Cystic RCC, Bosniak category IV (27)	2.68 ± 0.11
Angiomyolipoma (32)	2.13 ± 0.08
Oncocytoma (25)	2.26 ± 0.06
Renal abscess (16)	3.30 ± 0.07

map was registered consistent with the color by visual assessment. In the above-mentioned study, four to six oval regions of ROIs were placed over the renal masses on the ADC maps. These ROIs included a large ones encompassing as much of the mass as possible but excluding normal kidney parenchyma. In addition, small ROIs with a minimum area of 1 cm^2 were placed in the center and along the periphery of the mass. In another study, Rosenkrantz et al. have also used two-tier histologic grading system for ccRCC, and the DWI MR scanning was performed with the similar parameters that we had used. Authors received statistically significant difference in the mean ADC values for the low- and high-grade tumors: $1.85 \pm 0.40 \times 10^{-3}$ and $1.28 \pm 0.48 \times 10^{-3}$ mm^2/s, respectively ($p < 0.001$). For this measurement, the mean ADC was recorded within a round ROI placed on the ADC map within a portion of the tumor demonstrating visually low ADC [17]. The data obtained in the above-mentioned study correlate with data demonstrated in this trial and also correspond to our previous investigation which was limited to ccRCC histologic subtype only [18].

In 2014, Lassel et al. executed the meta-analysis that was based on 17 studies with 764 patients and demonstrated that RCCs have significantly lower ADC values than benign tissue ($1.61 \pm 0.08 \times 10^{-3}$ vs. $2.10 \pm 0.09 \times 10^{-3}$ mm^2/s; $p < 0.0001$). There was a significant difference between ADC values of RCCs and oncocytomas ($1.61 \pm 0.08 \times 10^{-3}$ vs. $2.00 \pm 0.08 \times 10^{-3}$ mm^2/s; $p < 0.0001$). Heterogeneity of the analyzed ADC values was a major limitation of this study [19].

Recent meta-analysis was performed in 2016 by Zhang et al. and included 11 subsets of data, and a total of 988 ADC measurements showed statistically significant ($p < 0.001$) differences in ADC values between benign lesions ($2.47 \pm 0.81 \times 10^{-3}$ mm^2/s) and malignant lesions ($1.81 \pm 0.41 \times 10^{-3}$ mm^2/s). The authors recommend that DW-MRI should be performed with a maximum b value ranging from 800 to 1000 s/mm^2 at 3.0 T for imaging protocol [20]. In our trial, we observed similar tendency in numbers as in the above-mentioned meta-analyses, but there were minor differences in mean ADC values of the normal healthy parenchyma, RCCs, and benign lesions in comparison with those studies. At the same time, both meta-analyses contain no data on histologic subtypes of RCC and on Fuhrman grades of differentiation.

Our study had some limitations: The wider spectrum of the ADC values of rare histologic subtypes of malignant and benign renal tumors as well as of the cysts of Bosniak categories I, II, IIF, and III should be analyzed in order to elaborate the full-scale algorithm for the differential diagnosis of RCC. Further investigation is required for the assessment of small renal lesions, benign complicated, and hemorrhagic renal cysts, and more cases of cystic RCC of different Fuhrman grades and lipid-poor AML are needed for appropriate statistical data analysis in these subgroups of patients.

Conclusion

The data received in our study demonstrate a substantial restriction of diffusion of hydrogen molecules in tissues of ccRCC in comparison with the healthy renal parenchyma preconditioned by the greater density of tumor. A statistically significant difference in mean ADC values of ccRCC with different grades of nuclear pleomorphism by Fuhrman was observed: Low-grade tumors showed higher mean

Table 3 Comparison of the ADC values between the normal renal parenchyma, cysts and tumors of different histologic subtypes and grades

Comparison	Mean ADC value ($\times 10^{-3}$ mm^2/s)	p value
Normal renal parenchyma versus solid RCC	2.47 ± 0.12 versus 1.63 ± 0.29	<0.01
Normal renal parenchyma versus cystic RCC	2.47 ± 0.12 versus 2.68 ± 0.11	<0.05
Normal renal parenchyma versus AML	2.47 ± 0.12 versus 2.13 ± 0.08	<0.05
Normal renal parenchyma versus OC	2.47 ± 0.12 versus 2.26 ± 0.06	<0.05
Normal renal parenchyma versus AB	2.47 ± 0.12 versus 3.30 ± 0.07	<0.01
Solid RCC versus cystic RCC	1.63 ± 0.29 versus 2.68 ± 0.11	<0.01
ccRCC grade I versus ccRCC grade II	1.92 ± 0.11 versus 1.84 ± 0.14	<0.05
ccRCC grade I versus ccRCC grade III	1.92 ± 0.11 versus 1.79 ± 0.10	<0.05
ccRCC grade I versus ccRCC grade IV	1.92 ± 0.11 versus 1.72 ± 0.06	<0.05
ccRCC grade II versus ccRCC grade III	1.84 ± 0.14 versus 1.79 ± 0.10	<0.05
ccRCC grade II versus ccRCC grade IV	1.84 ± 0.14 versus 1.72 ± 0.06	<0.05
ccRCC grade III versus ccRCC grade IV	1.79 ± 0.10 versus 1.72 ± 0.06	<0.05
ccRCC grade I versus pRCC	1.92 ± 0.11 versus 1.61 ± 0.07	<0.05
ccRCC grade II versus pRCC	1.84 ± 0.14 versus 1.61 ± 0.07	<0.05
ccRCC grade III versus pRCC	1.79 ± 0.10 versus 1.61 ± 0.07	<0.05
ccRCC grade IV versus pRCC	1.72 ± 0.06 versus 1.61 ± 0.07	<0.05
ccRCC grade I versus chRCC	1.92 ± 0.11 versus 1.46 ± 0.09	<0.05
ccRCC grade II versus chRCC	1.84 ± 0.14 versus 1.46 ± 0.09	<0.05
ccRCC grade III versus chRCC	1.79 ± 0.10 versus 1.46 ± 0.09	<0.05
ccRCC grade IV versus chRCC	1.72 ± 0.06 versus 1.46 ± 0.09	<0.05
ccRCC grade I versus cystic RCC	1.92 ± 0.11 versus 2.68 ± 0.11	<0.01
ccRCC grade II versus cystic RCC	1.84 ± 0.14 versus 2.68 ± 0.11	<0.01
ccRCC grade III versus cystic RCC	1.79 ± 0.10 versus 2.68 ± 0.11	<0.01
ccRCC grade IV versus cystic RCC	1.72 ± 0.06 versus 2.68 ± 0.11	<0.01
ccRCC grade I versus AML	1.92 ± 0.11 versus 2.13 ± 0.08	<0.05
ccRCC grade II versus AML	1.84 ± 0.14 versus 2.13 ± 0.08	<0.05
ccRCC grade III versus AML	1.79 ± 0.10 versus 2.13 ± 0.08	<0.05
ccRCC grade IV versus AML	1.72 ± 0.06 versus 2.13 ± 0.08	<0.01
ccRCC grade I versus OC	1.92 ± 0.11 versus 2.26 ± 0.06	<0.05
ccRCC grade II versus OC	1.84 ± 0.14 versus 2.26 ± 0.06	<0.05
ccRCC grade III versus OC	1.79 ± 0.10 versus 2.26 ± 0.06	<0.05
ccRCC grade IV versus OC	1.72 ± 0.06 versus 2.26 ± 0.06	<0.01
ccRCC grade I versus AB	1.92 ± 0.11 versus 3.30 ± 0.07	<0.01
ccRCC grade II versus AB	1.84 ± 0.14 versus 3.30 ± 0.07	<0.01
ccRCC grade III versus AB	1.79 ± 0.10 versus 3.30 ± 0.07	<0.01
ccRCC grade IV versus AB	1.72 ± 0.06 versus 3.30 ± 0.07	<0.01
pRCC versus chRCC	1.61 ± 0.07 versus 1.46 ± 0.09	<0.05
pRCC versus cystic RCC	1.61 ± 0.07 versus 2.68 ± 0.11	<0.01
pRCC versus AML	1.61 ± 0.07 versus 2.13 ± 0.08	<0.05
pRCC versus OC	1.61 ± 0.07 versus 2.26 ± 0.06	<0.05
pRCC versus AB	1.61 ± 0.07 versus 3.30 ± 0.07	<0.01
chRCC versus cystic RCC	1.46 ± 0.09 versus 2.68 ± 0.11	<0.01
chRCC versus AML	1.46 ± 0.09 versus 2.13 ± 0.08	<0.01
chRCC versus OC	1.46 ± 0.09 versus 2.26 ± 0.06	<0.01
chRCC versus AB	1.46 ± 0.09 versus 3.30 ± 0.07	<0.01
Cystic RCC versus AML	2.68 ± 0.11 versus 2.13 ± 0.08	<0.05
Cystic RCC versus OC	2.68 ± 0.11 versus 2.26 ± 0.06	<0.05
Cystic RCC versus AB	2.68 ± 0.11 versus 3.30 ± 0.07	<0.01
AML versus OC	2.13 ± 0.08 versus 2.26 ± 0.06	<0.05
AML versus AB	2.13 ± 0.08 versus 3.30 ± 0.07	<0.01
OC versus AB	2.26 ± 0.06 versus 3.30 ± 0.07	<0.01

ADC values compared to high-grade tumors. The modality of the MRI DWI along with ADC measurement allows to reliably differentiate between the solid RCC of main histologic subtypes and grades, cystic RCC, and the benign renal lesions.

Compliance with ethical standards

Conflict of interest The authors declare that they have no conflict of interest.

References

1. Jemal A, Siegel R, Ward E, Hao Y, Xu J, Thun MJ (2009) Cancer statistics, 2009. CA Cancer J Clin 59:225–249
2. Cheville JC, Lohse CM, Zincke H, Weaver AL, Blute ML (2003) Comparisons of outcome and prognostic features among histologic subtypes of renal cell carcinoma. Am J Surg Pathol 27:612–624
3. Miguel V, Fernando L, Carlos M et al (2009) Nuclear grade prediction of renal cell carcinoma using contrasted computed tomography. J Urol 181:249
4. Kim JK, Kim TK, Ahn HJ, Kim CS, Kim KR, Cho KS (2002) Differentiation of subtypes of renal cell carcinoma on helical CT scans. AJR Am J Roentgenol 178:1499–1506
5. Sheir KZ, El-Azab M, Mosbah A, El-Baz M, Shaaban AA (2005) Differentiation of renal cell carcinoma subtypes by multislice computerized tomography. J Urol 174:451–455
6. Moinzadeh A, Gill IS, Finelli A, Kaouk J, Desai M (2006) Laparoscopic partial nephrectomy: 3-year followup. J Urol 175:459–462
7. Le Bihan D (1991) Molecular diffusion nuclear magnetic resonance imaging. Magn Reson 7:1–30
8. Pedrosa I, Sun MR, Spencer M, Genega EM, Olumi AF, Dewolf WC, Rofsky NM (2008) MR imaging of renal masses: correlation with findings at surgery and pathologic analysis. Radiographics 28:985–1003
9. Taouli B, Thakur RK, Mannelli L, Babb JS, Kim S, Hecht EM, Lee VS, Israel GM (2009) Renal lesions: characterization with diffusion-weighted imaging versus contrast-enhanced MR imaging. Radiology 251:398–407
10. Sandrasegaran K, Sundaram CP, Ramaswamy R, Akisik FM, Rydberg MP, Lin C, Aisen AM (2010) Usefulness of diffusion-weighted imaging in the evaluation of renal masses. AJR Am J Roentgenol 194:438–445
11. Kanal E (2016) Gadolinium based contrast agents (GBCA): safety overview after 3 decades of clinical experience. Magn Reson Imaging. doi:10.1016/j.mri.2016.08.017
12. McDonald RJ, McDonald JS, Bida JP, Carter RE, Fleming CJ, Misra S, Williamson EE, Kallmes DF (2016) Intravenous contrast material-induced nephropathy: causal or coincident phenomenon? Radiology 278:306
13. Wang H, Cheng L, Zhang X, Wang D, Guo A, Gao Y, Ye H (2010) Renal cell carcinoma: diffusion-weighted mr imaging for subtype differentiation at 3.0 T. Radiology 257:135–143
14. Razek AA, Farouk A, Mousa A, Nabil N (2011) Role of diffusion-weighted magnetic resonance imaging in characterization of renal tumors. J Comput Assist Tomogr 35:332–336
15. Sun M, Lughezzani G, Jeldres C, Isbarn H, Shariat SF, Arjane P, Widmer H, Pharand D, Latour M, Perrotte P, Patard JJ, Karakiewicz PI (2009) A proposal for reclassification of the Fuhrman grading system in patients with clear cell renal cell carcinoma. Eur Urol 56:775–781
16. Hong SK, Jeong CW, Park JH, Kim HS, Kwak C, Choe G, Kim HH, Lee SE (2011) Application of simplified Fuhrman grading system in clear-cell renal cell carcinoma. BJU Int 107:409–415
17. Rosenkrantz AB, Niver BE, Fitzgerald EF, Babb JS, Chandarana H, Melamed J (2010) Utility of the apparent diffusion coefficient for distinguishing clear cell renal cell carcinoma of low and high nuclear grade. AJR Am J Roentgenol 195:W344–W351
18. Mytsyk Y, Borys Y, Komnatska I, Dutka I, Shatynska-Mytsyk I (2014) Value of the diffusion-weighted MRI in the differential diagnostics of malignant and benign kidney neoplasms—our clinical experience. Pol J Radiol 79:290–295
19. Lassel EA, Rao R, Schwenke C, Schoenberg SO, Michaely HJ (2014) Diffusion-weighted imaging of focal renal lesions: a meta-analysis. Eur Radiol 24:241–249
20. Zhang H, Gan Q, Wu Y, Liu R, Liu X, Huang Z, Yuan F, Kuang M, Song B (2016) Diagnostic performance of diffusion-weighted magnetic resonance imaging in differentiating human renal lesions (benignity or malignancy): a meta-analysis. Abdom Radiol (NY) 41:1997–2010